Front. Earth Sci. 2021, 15(2): 256–271
https://doi.org/10.1007/s11707-021-0917-6

RESEARCH ARTICLE

Coalbed methane enrichment model of low-rank coals in multi-coals superimposed regions: a case study in the middle section of southern Junggar Basin

Haihai HOU (✉)[1,2], Guodong LIANG[1], Longyi SHAO (✉)[2], Yue TANG[3], Guangyuan MU[2]

1 College of Mining, Liaoning Technical University, Fuxin 123000, China
2 College of Geoscience and Surveying Engineering, China University of Mining and Technology, Beijing 100083, China
3 Oil & Gas Resource Survey Center, China Geological Survey, Ministry of Land and Resource, Beijing 100029, China

Abstract The Middle Jurassic Xishanyao Formation in the central section of the southern Junggar Basin has substantial amounts of low-ranked coalbed methane (CBM) recourses and is typically characterized by multi superimposed coal seams. To establish the CBM enrichment model, a series of experimental and testing methods were adopted, including coal maceral observation, proximate analysis, low temperature nitrogen adsorption (LTNA), methane carbon isotope determination, porosity/permeability simulation caused by overburden, and gas content testing. The controlling effect of sedimentary environment, geological tectonic, and hydrogeological condition on gas content was analyzed in detail. The results demonstrate that the areas with higher gas content (an average of 8.57 m^3/t) are mainly located in the Urumqi River-Santun River (eastern study area), whereas gas content (an average of 3.92 m^3/t) in the Manasi River-Taxi River (western study area) is relatively low. Because of the combined effects of strata temperature and pressure, the gas content in coal seam first increases and then decreases with increasing buried depth, and the critical depth of the inflection point ranges from 600 m to 850 m. Affected by the changes in topography and water head height, the direction of groundwater migration is predicted from south to north and from west to east. Based on the gas content variation, the lower and middle parts of the Xishanyao Formation can be divided into three independent coal-bearing gas systems. Within a single gas-bearing system, there is a positive correlation between gas content and strata pressure, and the key mudstone layers separating each gas-bearing system are usually developed at the end of each highstand system tract. The new CBM accumulation model of the multi-coals mixed genetic gas shows that both biological and thermal origins are found in a buried depth interval between 600 m and 850 m, suggesting that the coals with those depths are the CBM enrichment horizons and favorable exploration regions in the middle section of the southern Junggar Basin. An in-depth discussion of the low-rank CBM enrichment model with multi-coal seams in the study region can provide a basis for the optimization of CBM well locations and favorable exploration horizons.

Keywords Xishanyao Formation, multi-coal seams superimposed region, low rank coal, main controlling factors, enrichment model

1 Introduction

Coalbed methane (CBM) is a type of unconventional natural gas mainly stored in coal seams. It has garnered the attention of the related scientists and policy makers owing to increasing global energy consumption. The effective development and utilization of CBM resources are of great significance for optimizing the energy industrial structure, cutting greenhouse gas emissions, reducing air pollution, and addressing coal mine safety issues (Moore, 2012; Qin et al., 2018). The low rank CBM in China has vast potential for exploration and development; however, the production yield of low rank CBM wells currently only accounts for approximately 5% (Zou et al., 2015). The maximum vitrinite reflectance ($R_{o,max}$) of the Middle Jurassic Xishanyao Formation in the southern margin of the Junggar Basin ranges from 0.41% to 0.74% (Hou et al., 2019). Although the Xishanyao Formation of the Middle Jurassic in the southern Junggar Basin has abundant low

Received February 2, 2021; accepted June 10, 2021

E-mails: houmensihai@163.com (Haihai HOU), shaol@cumtb.edu.cn (Longyi SHAO)

rank CBM resources, a breakthrough in CBM exploitation is rare likely due to the lack of understanding of the CBM enrichment law and its main controlling factors (Li et al., 2018b; Yuan et al., 2020). Therefore, an in-depth study on CBM accumulation patterns in the southern Junggar Basin will be conducive to further CBM exploration and development.

Many factors affect the gas content in coal seams, including coal lithotypes, coal seam thickness, coal seam temperature and pressure, coal seam depth, roof and floor lithology, structural evolution, and hydrogeological condition (Cienfuegos and Loredo, 2010; Li, 2016; Ouyang et al., 2017). Based on previous investigations, the factors influencing CBM enrichment can be summarized as sedimentary environment, geologic structure, hydrogeology, and coal reservoir physical property (Shao et al., 2015; Fu et al., 2016). However, for different CBM blocks and different rank coals, there are various dominant factors affecting CBM enrichment. The influence of burial depth on CBM occurrence is mainly characterized by changes in the strata temperature and pressure. Under the same reservoir temperature/pressure and the similar coal structure, the adsorption capacity of coal seams generally becomes stronger from low rank coals to high rank coals (Li et al., 2014a; Wang, 2019). However, a high gas content does not always mean high gas production, and there are many blocks with sufficient gas supply but extremely low gas yield (Pan et al., 2015; Hou et al., 2017). As another significant factor, hydrogeological conditions not only affect the generation of low rank CBM but also have an important impact on the CBM preservation for both low-rank and high-rank coals (Hamilton et al., 2012; Lv et al., 2012; Yao et al., 2014). Considering the depositional environments, structural characteristics, hydrogeology, lithology, and in situ stress, previous researchers have generally categorized the CBM enrichment modes into four types: closed pressure type, confined water plugging type, network microfiltration plugging type under roof water, and structural trap type (Ayers, 2002; Chen et al., 2015; Chen et al., 2019). For low rank coals, based on biological effects, geological tectonics, hydrodynamic and lithological characteristics, CBM enrichment models can be divided into four types: deep pressure-bearing type, gentle slope biological effect type at the edge of the basin, hydrodynamic plugging type of conventional traps at structural high points, and broad gentle fold type (Liu et al., 2018; Li et al., 2019). For medium-high rank coals, based on the differences in structural features, hydrodynamic conditions, strata stress, and pore-fracture development, the CBM enrichment regions can be summarized into five types, including slope area with the superior superposition of gas content and permeability, brittle-ductile transition zone, relatively high structure area, gentle zone, and rift zone (Yang et al., 2015; Song et al., 2016).

In terms of the southern margin of the Junggar Basin, four CBM enrichment models were identified according to hydrodynamic conditions, burial depth, CBM genesis, and migration types: 1) an autogenous CBM model containing biogenic adsorbed gas in shallow coal seams, 2) an endogenous migration model containing thermogenic adsorbed gas in mid-deep coal seams, 3) an exogenous migration model containing thermogenic adsorbed gas in deep coal seams, and 4) an exogenous migration model containing thermogenic free and adsorbed gas in ultra-deep coal seams (Fu et al., 2017; Li et al., 2018a). Although several investigations on the enrichment regularity and pattern of CBM in the study area have been conducted, there is still a lack of targeted and effective CBM enrichment models in the multi-coal superimposed areas. Based on the analyses of CBM geology and sequence stratigraphy, this study focused on the CBM enrichment law and its dominant factors of the Middle Jurassic Xishanyao Formation in the southern Junggar coalfield. A new CBM enrichment model was finally established in the multi-coal seams superimposed regions, which not only provides a new perspective for the evaluation of CBM favorable regions in the middle section of the southern Junggar Basin, but also has a certain guiding significance for further breakthroughs in exploration and development.

2 Geological setting

2.1 Tectonic characteristics

The southern Junggar Basin belongs to the faulted and folded areas of the North Tian Mountains in northwestern China, with the surrounding areas mostly outcropped by Paleozoic strata. Specifically, it is a part of the multi-period superimposed and inherited structural belt of the foreland basin, which has experienced multiple tectonic movements covering the Hercynian, Indosinina, Yanshan, and Himalayan (Scheltens et al., 2015). The study area is situated in the middle section of southern Junggar Basin, reaching Manas River in the west, Miquan County in the east, and the boundary fault to the south (Fig. 1). Monoclines and folds were well developed from the boundary fault to the basin direction. Furthermore, a large left-lateral Urumqi-Miquan strike-slip fault formed during the late Indosinian movement was found in the eastern part of the study area (Sun and Shen, 2014; Fu et al., 2019). Thus, the structural types of coal-bearing strata in the study area are mainly anticlines, synclines, and monoclines in the west, and strike-slip faults in the east. The southern Junggar Basin is influenced by strong north–south compressional geological movement, which results in a complex geo-stress field (Fu et al., 2020). Affected by the uplift of the North Tian Mountains in the western part of the study area, the maximum horizontal stress direction is approximately north–south, which shows NW14° in the Hutubi anticline (Li et al., 2005). Owing to the dual action of the North Tian

Mountains and the Bogda Mountains uplift in the eastern area, the maximum horizontal stress direction slightly shifts to the northwest with NW35° (Li et al., 2005; Fig. 1).

2.2 Coal-bearing strata and sedimentary environment

The Jurassic coal-bearing strata in the southern Junggar Basin consist of the Lower Jurassic Badaowan Formation and Sangonghe Formation, together with the Middle Jurassic Xishanyao Formation from bottom to top. Among them, the Xishanyao Formation is the main coal- bearing strata in the middle section of the southern Junggar Basin. The lithologies in the Xishanyao Formation are mainly composed of sandstone, siltstone, mudstone, and coal. The coal-accumulating centers can be predicted in the Manas area (western study area) and the Liuhuanggou area (eastern study area) (Li et al., 2018b). In the western region, multi-layer coal seams are developed with an average thickness of 39.62 m. Compared with the west, the coal layers in the eastern region are relatively few, but the individual coal seam is relatively thick, with an average thickness of 32.19 m. The coal-bearing strata of the Xishanyao Formation in the southern Junggar Basin were formed in the early period of the Middle Jurassic, which was mainly deposited in fan delta, braided river delta, and lacustrine environments (Chen et al., 2014; Hou et al., 2021).

2.3 Regional hydrogeology

Combined with the vertical distribution of the inflow and leakage water during the drilling process in several CBM wells, three major aquifers in the Xishanyao Formation can be identified. These aquifers highly coincide with the bottom boundary of the third-order sequences, and they are located at the base of each lowstand system tract (Fig. 2). This is because the sandstone layer with scouring surface usually shows a relatively coarse lithology and is subject to relatively strong hydrodynamic conditions (Fig. 2). Overall, the vertically developed aquifers are controlled by the sequence stratigraphic framework to some degree for the Xishanyao Formation in the southern Junggar Basin.

3 Experimental and research methods

The field and laboratory approaches in this study include proximate analysis, coal maceral observation, low-temperature nitrogen adsorption (LTNA), methane carbon isotope determination, simulation of overburden porosity/permeability, and gas content testing.

1) Proximate analysis and coal maceral observation

Proximate analyses of coal samples were carried out by the Unconventional Petroleum Service of SGS-CSTC Standards Technical Services Co., Ltd (UPS-SGS),

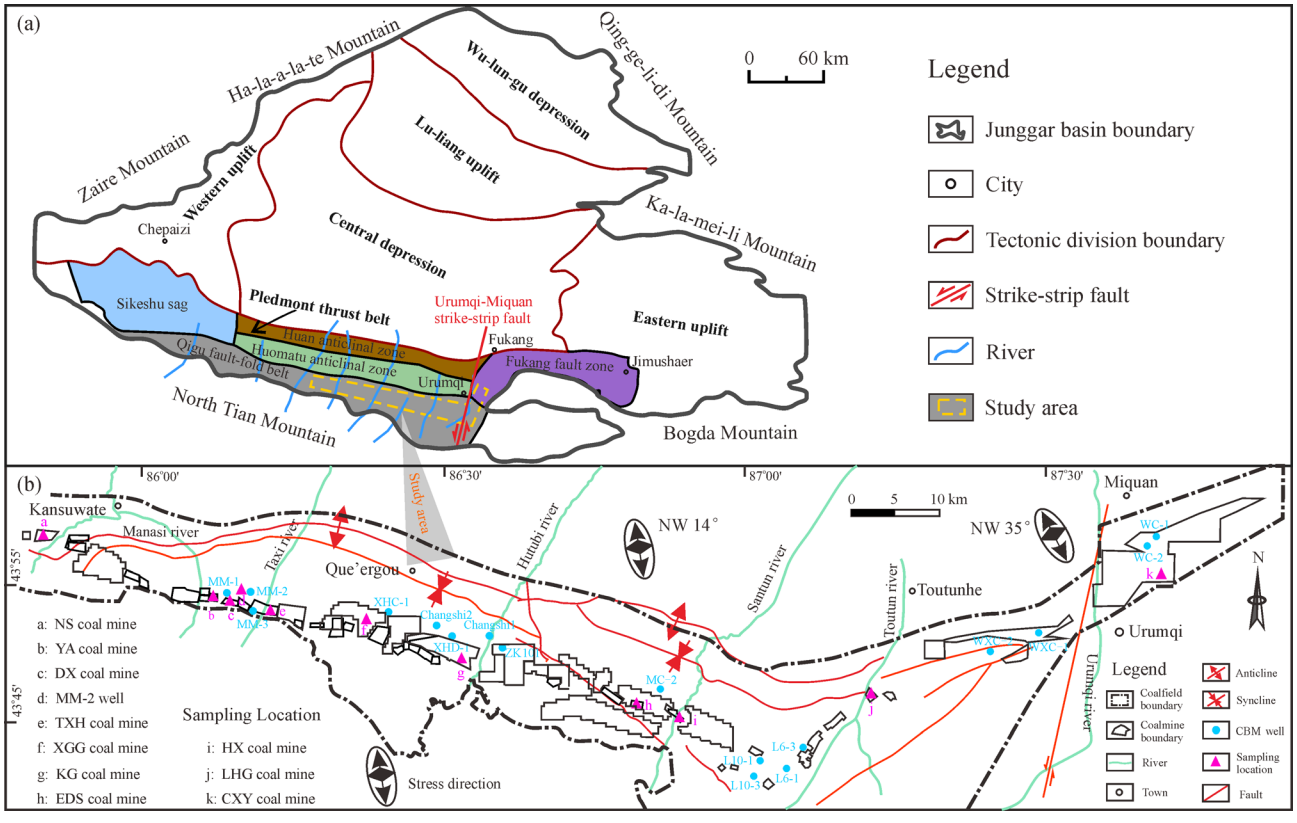

Fig. 1 (a) Geotectonic sketch map of the Junggar Basin. (b) Structural characteristics of the study area showing the locations of CBM wells, coal mines, coal samples and horizontal maximum stress directions.

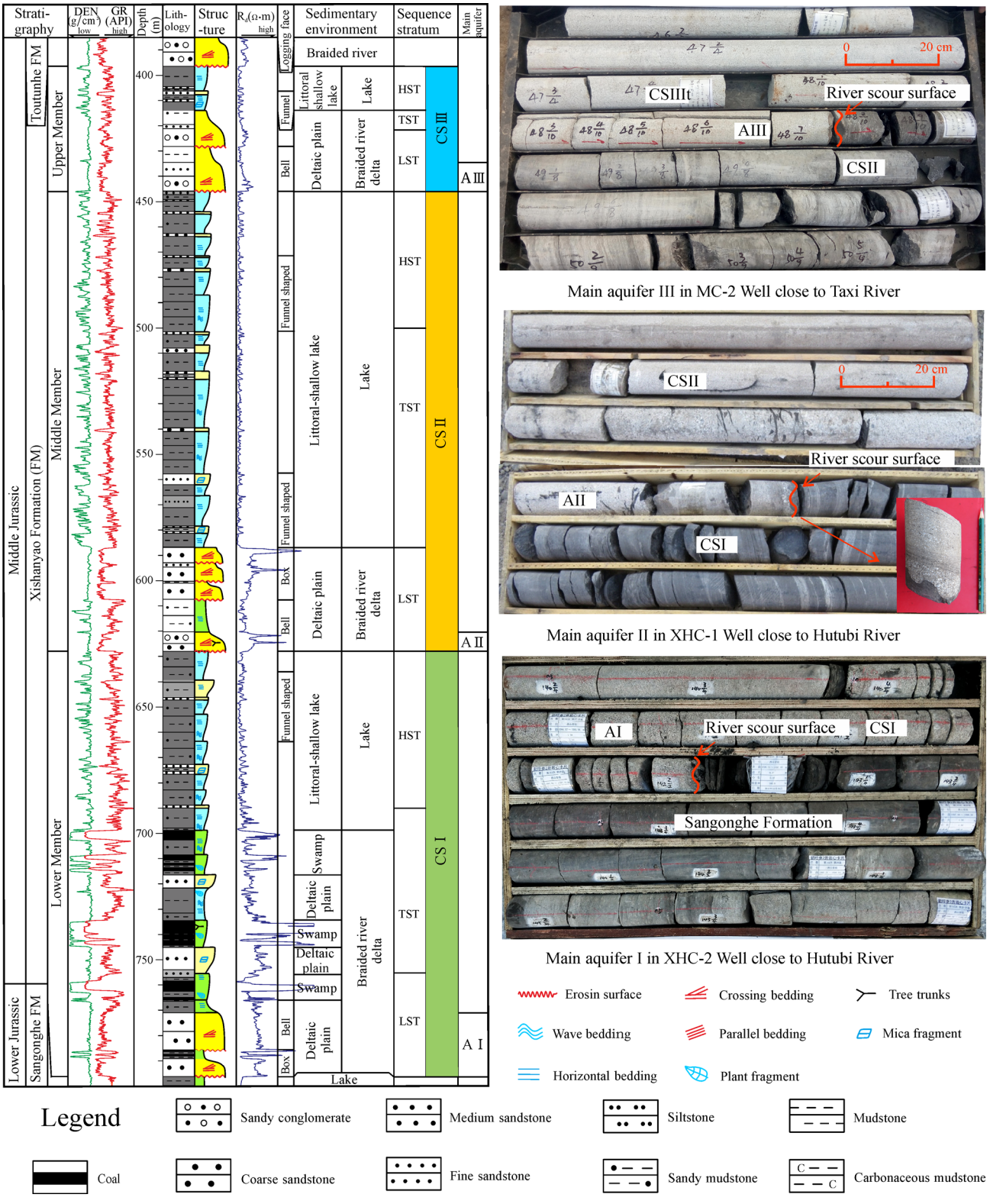

Fig. 2 The coal-bearing strata of the Middle Jurassic Xishanyao Formation showing lithology, depositional environment, sequence stratum, core pictures and main aquifers in Well ZK101 close to Hutubi River.

following the National Standard GB/T 30732-2014. The relevant data for parameters such as ash yield, moisture content, volatile component, and fixed carbon content were obtained. In accordance with the National Standard GB/T 8899-1998, coal macerals were quantitatively observed at the Geological Laboratory of Liaoning Technical University, and the volume proportions of vitrinite, inertinite, and exinite within each sample were obtained.

2) Low temperature nitrogen adsorption (LTNA)

According to the National Petroleum Industry Standard SY/T 6154-1995, the LTNA experiment was performed using a Quantachrome NOVA 2000E specific surface area and pore diameter distribution analyzer at UPS-SGS. After being dried at 105°C for 8 h, each sample (5–10 g) was crushed to 40–60 mesh (0.42–0.28 mm size) for testing. For each specimen, the nitrogen adsorption-desorption isotherm was charted at 77 K with a relative pressure of 0.01–0.99. The pore volume and specific surface area were obtained using the BJH (Barrett-Joyner-Halenda) model and BET (Brunauer-Emmett-Teller) model, respectively.

3) Gas content and methane carbon isotope

The gas content of coals was tested through rope coring from several CBM parameter wells. The total gas content is the summation of desorption gas, loss gas, and residual gas. The amount of residual gas was determined at the Gas Geological Institute of Henan Polytechnic University. The stable carbon isotope in the desorbed gas was analyzed using a MAT-253 gas isotope ratio mass spectrometer (IRMS) by UPS-SGS according to the Chinese National Standard GB/T 18340.2-2010 with an instrument accuracy of ±0.2 (PDB).

4) Porosity and permeability simulation by overburden

The porosity and permeability simulation method under overburden pressure was conducted at the Research Institute of Petroleum Exploration and Development, based on the Petroleum and Natural Gas Industry Standard SY/T 6385-1999. In this experiment, the CMS-300 overburden pressure porosity-permeability automatic tester was controlled using a computer. Under a series of overburden pressures up to 10000 psi, the porosity and permeability of the coal samples were directly measured, and the testing permeability ranged from 0.0001 mD to 10 D.

5) Research methods

The influencing factors for the CBM enrichment rule of the Middle Jurassic Xishanyao Formation in the southern Junggar Basin were analyzed from three aspects: sedimentation, geological structure, and hydrogeological condition. Given these aspects, sedimentary factors covering coal thickness, coal quality, coal maceral, and the roof and floor lithology of coal seams were investigated. As the geologic structure has a great impact on the macroscopic fractures and permeability of coal seam, the influences of different structure types and different magnitudes (directions) of *in situ* stress on coal permeability were chiefly investigated. Hydrogeological parameters, including reservoir pressure, salinity, head height, and water-rich center, were analyzed to establish the CBM enrichment model in multiple coal-developed regions.

4 Results and discussion

4.1 Variations of gas content in the research region

To clarify the gas content variations and their controlling factors, a total of 165 gas content data sourcing from the underground coal mines and the CBM parameter wells were analyzed (Fig. 3). The gas content in the Xishanyao coals is distributed between 0.24 m^3/t and 17.06 m^3/t. Specifically, gas contents in most areas are less than 5 m^3/t (Table 1; Fig. 3), and the highest value is found in the Urumqi River-Santun River (eastern region). Owing to the combined effects of reservoir temperature and pressure, the gas content of the Xishanyao coals in the study area first increases and then decreases with increasing buried depth, and the critical depth corresponding to the gas inflection point is between 600 m and 850 m (Fig. 3). Among these data, the maximum gas content is 17.06 m^3/t, occurring in the B6 coal seam of the WXC-1 well, and its corresponding buried depth is 614 m, which can be attributed to both thermogenic gas and biogenic gas. This inference is based on the confirmation of the presence of biogenic gas in this region (Fu et al., 2019). Overall, the gas content variation with the buried depth shallower than 600 m is mainly controlled by the positive effect of reservoir pressure, just with an average value of 2.22 m^3/t. The buried depth ranges from 600 m to 850 m, and the average gas content is 4.10 m^3/t. When the buried depth range is between 850 m and 1411 m, the gas content is likely controlled by the negative effect of reservoir temperature with an average of 3.24 m^3/t, thus a decreasing trend in gas content is observed with increasing coal depth (Song et al., 2012).

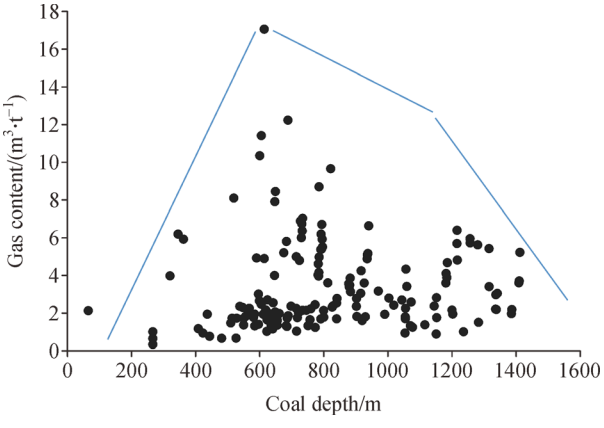

Fig. 3 Gas content variation of the Xishanyao coals in the middle part of southern Junggar Basin.

Table 1 The well testing data, gas content, roof and floor lithology of major coal seams in several CBM parameter wells, southern Junggar Basin

Well	Coal seam	Burial depth/m	Reservoir pressure/MPa	Pressure gradient/ (kPa·m^{-1})	Permeability/mD	Gas content/ (m^3·t^{-1})	Roof lithology	Floor lithology
WXC-1	B7	396.14	2.85	7.8	7.28	11.33	Silty mudstone	Mudstone
	B6	613.7	5.15	8.65	0.13	17.06	Muddy siltstone	Mudstone
WXC-2	B8	546.95	3.96	7.55	0.16	4.53	Muddy siltstone	Silty mudstone
	B7	589.15	5.76	10	14.49	4.93	Medium sandstone	Siltstone
	B5	714.45	4.93	7.04	9.92	5.0	Muddy siltstone	Mudstone
MM-1	B10	1056.8	10.51[a)]	n	n	3.33	Silty mudstone	Siltstone
	B5	1183	11.98[a)]	n	n	4.07	Silty mudstone	Mudstone
	B2	1256.2	12.84[a)]	n	n	5.95	Silty mudstone	Mudstone
MM-2	B10	1185.68	12.21	10.3	1.929	1.82	Coarse sandstone	Mudstone
	B5	1388.23	14.02	10.1	0.269	2.61	Silty mudstone	Siltstone
	B2	1473.86	15.18	10.3	0.004	4.18	Mudstone	Silty mudstone
MM-3	B9	784.04	7.84	9.9	0.024	4.35	Muddy siltstone	Mudstone
	B5	880.53	8.5	9.7	0.091	3.49	Muddy siltstone	Siltstone
	B2	939.88	10.43	11.1	0.027	5.45	Silty mudstone	Mudstone

Notes: n, no data; a) data were predicted based on the equation of $Y = 0.0117X–1.8569$, where Y is reservoir pressure and X is burial depth.

4.2 Influence of sedimentary environment on gas content

The influence of the sedimentary environment on CBM enrichment is mainly reflected in three aspects: 1) coal seam thickness and its distribution; 2) coal maceral, coal quality, and reservoir inhomogeneity; and 3) the lithology and thickness of the surrounding rocks (Hou et al., 2019). Generally, it is believed that the thicker the coal seam is, the higher the gas content it will yield (Fu et al., 2017). Additionally, coal seams with high vitrinite contents and low ash yields have relatively high gas contents (Hou et al., 2019). However, these features can be observed in the regions with the similar buried depths and the similar roof and floor lithologies (Yuan et al., 2020). Therefore, the lithology and thickness of the surrounding rock of the coal seams play more significant roles in influencing CBM accumulation than other sedimentary factors such as coal seam thickness, coal macerals, and coal property data.

4.2.1 Relationship between surrounding rock condition and gas content

Generally, oil shale, mudstone, and silty mudstone are more conducive for CBM storage than sandstone, sand-mud interbed, and carbonate (Hou et al., 2019). The roof and floor in the Xishanyao coal-bearing strata are mainly composed of sandstone, silty mudstone, argillaceous siltstone, and mudstone (Fig. 2). Owing to the relatively high densification, the permeability and porosity in mudstones are generally low (Li et al., 2020). When the mudstone content within the roof and floor is relatively high, the sealing property is better, which is beneficial for CBM preservation (Tang, 2020).

In this study, a drilling core description was carried out in Well XHC-1 with burial depths ranging from 1101.97 m to 822.92 m, and in Well MM-3 with depths ranging from 801.31 m to 656.28 m. The core observations specifically include the lithology and thickness of each layered section, depth, sedimentary structure, and sedimentary facies. The roof/floor lithological combination of the Xishanyao coals can be classified into the following four types:

In Type I, coal seam can be directly eroded by the overlying roof developed in a braided channel or delta distributary channel. The lithology of the roof usually shows thick middle-coarse grain sandstones, whereas the floor is mostly composed of mudstone or siltstone. In addition, as shown in Fig. 4 (Well XHC-1), most of the sandstone bottom has obvious erosion surfaces. The B3 coal seam in this lithology combination has the lowest gas content just with 2.05 m^3/t (Fig. 4). For Type II, the coal seam is mainly developed in the lakeshore swamp. Its roof is covered by the sand and mudstone interbeds deposited in the delta front, and the bottom of the coal seam is the lakeshore sand bar in the MM-3 well (Fig. 4). The gas content of the B5 coal seam in Type II is relatively low, with an average of 3.48 m^3/t (Fig. 4). Taking Type III in the MM-3 well as an example, the coal seam and its roof/floor are developed in the distributary bay of the lower deltaic plain. If the water level becomes shallow during the deposition process, a silty mudstone roof appears. The average gas content of the B9 coal seam in Type III lithologic combination is medium, with an average value

of 4.35m^3/t (Fig. 4). For Type IV, owing to the deeper water level, the roof and floor of the B7 coal seam show dark gray or gray-black mudstone, with the highest gas content of 9.66 m^3/t. Therefore, this type is beneficial for CBM preservation in the middle section of the southern Junggar Basin. However, in this study area, the roof and floor lithology combinations are mostly Type I and Type II, and the coal seams generally have low gas content. Therefore, it is necessary to further analyze the differences in porosity and permeability of these two types, seeking favorable horizons and supporting fracturing and drainage work.

4.2.2 Identification and division of multi-superimposed gas bearing system

The multi-superimposed gas bearing system, as a special form of CBM accumulation in the areas where multiple coal seams are developed, has been extensively concerned by many scholars in recent years owing to its significant implications for the distribution of strata energy and multi-layer drainage (Shen et al., 2017; Yuan et al., 2018). The variations in the pressure gradient and gas content in multi-coal layers are two important indicators that are often used to classify vertical gas-bearing systems (Table 1). As there are less data on pressure gradient, gas content data are mainly used to identify whether there are multiple vertical gas-bearing systems in the study area. In the MM-3 well, the gas content initially increases and then decreases with increasing buried depth (Fig. 5). Specifically, the relationship between gas content and buried depth can be divided into three stages. In each stage, the gas content increases with increasing buried depth up to the maximum value corresponding to the horizon with thick gray-black mudstone (Fig. 5).

Based on changes in the lithologic column, coal reservoir pressure, gas content, and sequence stratigraphic division of the MM-3 well, the Middle-Lower Xishanyao Formation of the well can be divided into three relatively independent vertical superimposed gas-bearing systems (Fig. 5). In the boundaries of three gas-bearing systems, the developed dark mudstone with a certain thickness can be found (Fig. 5), which results in the three vertically independent gas-bearing/water-bearing systems due to the low porosity and permeability characteristics. Therefore, the key strata dividing the multi-layered gas-bearing system in the southern Junggar Basin can be identified as thick gray-black mudstones with stable development in the region. Compared with the results of sequence stratigraphic division, these stable black mudstones are closely related to the development of sequence strata; the key strata are always developed near the maximum lake flooding level or in the late period of the lacustrine transgressive system tract. It is also worth noting that more gas systems should exist for the Xishanyao Formation considering the MM-3 well shown in Fig. 5, which lacks the upper segment. Combined with the data of specific surface area, total pore volume, and well test permeability, it is determined that there is no clear relationship between the variation in coal gas content and these three parameters (Fig. 5). Consequently, in a single gas-bearing system, the reservoir pressure (fluid pressure) plays a dominant role in controlling the variation of gas content in comparison with the permeability, specific surface area, and total pore volume of coals.

4.3 Influence of tectonic condition on gas content

Geological structures, as one of the key factors influencing low rank CBM accumulation, not only determine the development characteristics of coal-bearing measures, but also largely control CBM migration, accumulation, and preservation. Additionally, tectonic activity fundamentally affects the history of the sedimentary environment and the thermal evolution of coal-bearing measures. Therefore, CBM generation, occurrence, and accumulation show different characteristics under different structural conditions (Pashin and Groshong, 1998; Li et al., 2013).

The basic structural framework in the study area shows a large monocline inclined in the north direction, with a series of secondary faults and related folds (anticlines and synclines) (Fu et al., 2017). Owing to the compressional stress from south to north, the western part of the study area is mainly characterized by gas-controlling structures such as monoclines and anticlines (Fig. 6(a)) with a relatively large extrusion stress. Therefore, macroscopic fractures are not well-developed in this area, and the permeability is relatively low with an average of 0.391 mD (Figs. 6(b) and 6(c)). For the eastern part of the study area, a northeast to southwest trending strike-slip structure is superimposed on the existing north–south compressional tectonics, which partially releases the north–south extrusion stress. Thus, the macroscopic fractures in the eastern area are well-developed, and the coal permeability is relatively high with an average value of 6.396 mD (Fig. 6(d)). Based on the relevant results, the accumulation and seepage capacity of CBM show differences under various structural assemblages and geo-stresses (Chen et al., 2015; Xiao et al., 2015).

To analyze the changes in coal porosity and permeability with increasing strata pressure, five coal samples from KG1-1, XGG-1, TXH-1, TXH-2, and LHG-2 coal mines in the study area are selected to perform the porosity/permeability simulation of overburden (Fig. 7). With increasing overburden pressure from 5 MPa to 30 MPa, the coal porosities of KG1-1, XGG-1, TXH-1, TXH-2, and LHG-2 show a decreasing trend from 2.95% to 0.40%, 2.14% to 0.52%, 3.55% to 1.37%, 3.39% to 0.75%, and 0.61% to 0.04%, respectively. The coal permeabilities of the KG1-1, XGG-1, TXH-1, TXH-2, and LHG-2 decrease rapidly from 0.0090 mD to 0.0009 mD, 0.0104 mD to 0.0010 mD, 2.1700 mD to 0.0150 mD, 0.0470 mD to 0.0005 mD, and 0.0014 mD to 0.0002 mD, severally.

Fig. 4 Typcial surrounding rock combinations of Xishanyao coals in the middle part of southern Junggar Basin.

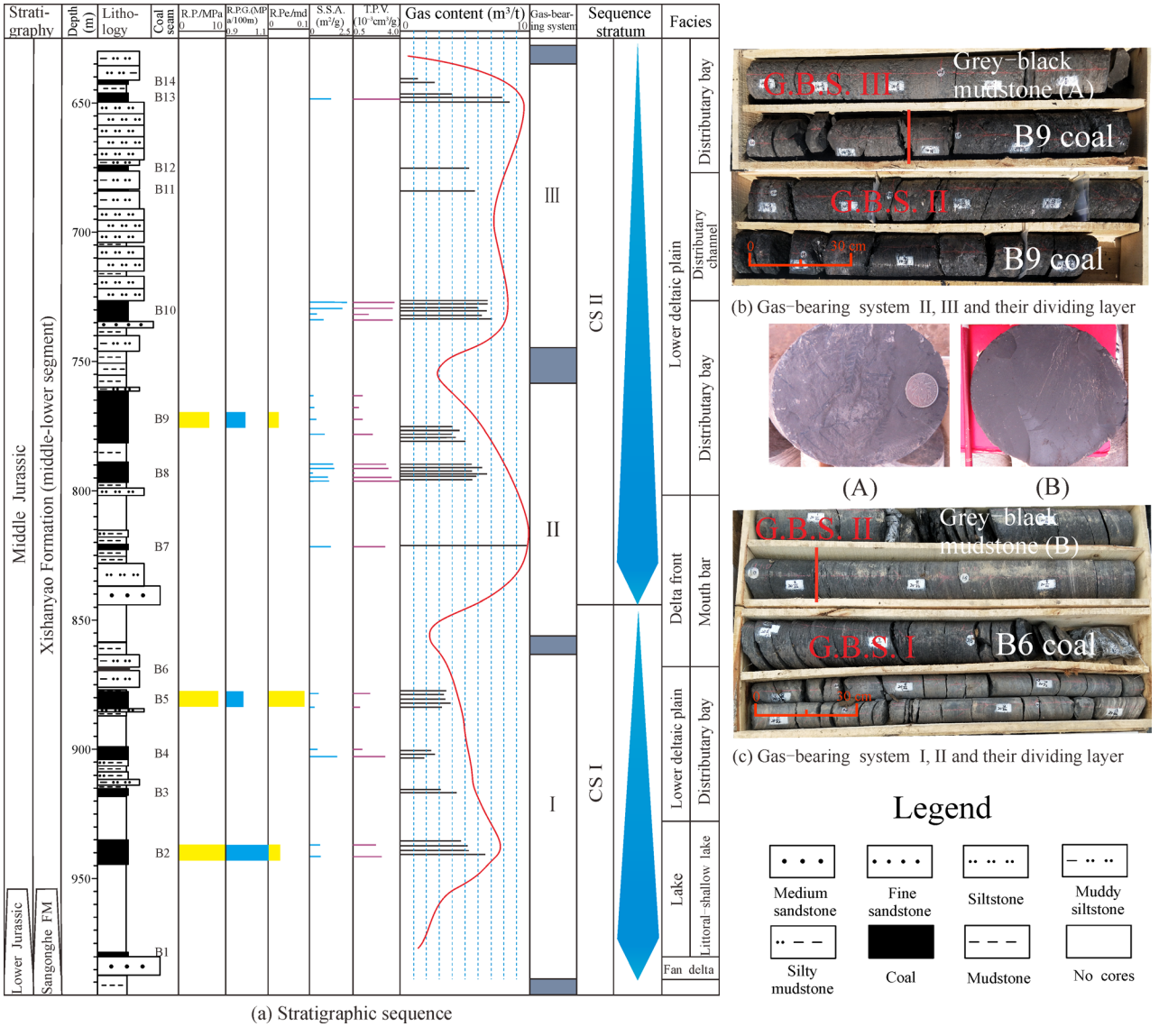

Fig. 5 The division of multi-superimposed gas system of the Xishanyao Formation in the MM-3 well (R.P.—Reservoir pressure; R.P.G.—Reservoir pressure gradient; R.Pe.—Reservoir permeability; S.S.A.—Specific surface area; T.P.V.—Total pore volume).

Based on the porosity/permeability simulation of overburden for the five coal samples, the following rules can be drawn: 1) The porosity and permeability of coals rapidly decrease as the pressure of the overlying strata increases; 2) Under the same burial depth and strata pressure, the porosity and permeability of coal samples from the Taxihe coal mine are the highest, whereas those from the Liuhuanggou coal mine are the lowest, which can be attributed to the differences in ash yields (Hou et al., 2020); 3) In the western regions, the coals near Taxihe were well-developed in mineral-trophic swamps, and the ash yields of coals are between 4.03% and 17.44% (an average of 11.29%). In contrast, those of the eastern areas vary from 2.24% to 8.36% (an average of 5.23%). It can be predicted that the western coals have high ash yields, more minerals, and strong compressive strengths, resulting in relatively high porosities and permeabilities under the same strata pressure. Overall, the structure types in the study area mainly consist of monocline, folds, and faults. The favorable enrichment of CBM is closely related to the syncline-enriched zone (Fu et al., 2017; Yuan et al., 2020). Generally, the CBM content shows an increasing trend from the two wings to the axis for a syncline structure. However, it should be noted that the negative effect of strata temperature needs to be considered for a buried depth greater than 850 m. For the eastern study area, due to the influence of strike-slip faults, the structure types not only affect the enrichment of CBM but also control the migration of CBM to a certain extent. The extensional deformation zone is beneficial for migration but not conducive to accumulation due to relatively low pressure; and the shrinkage zone shows a contrasting tendency.

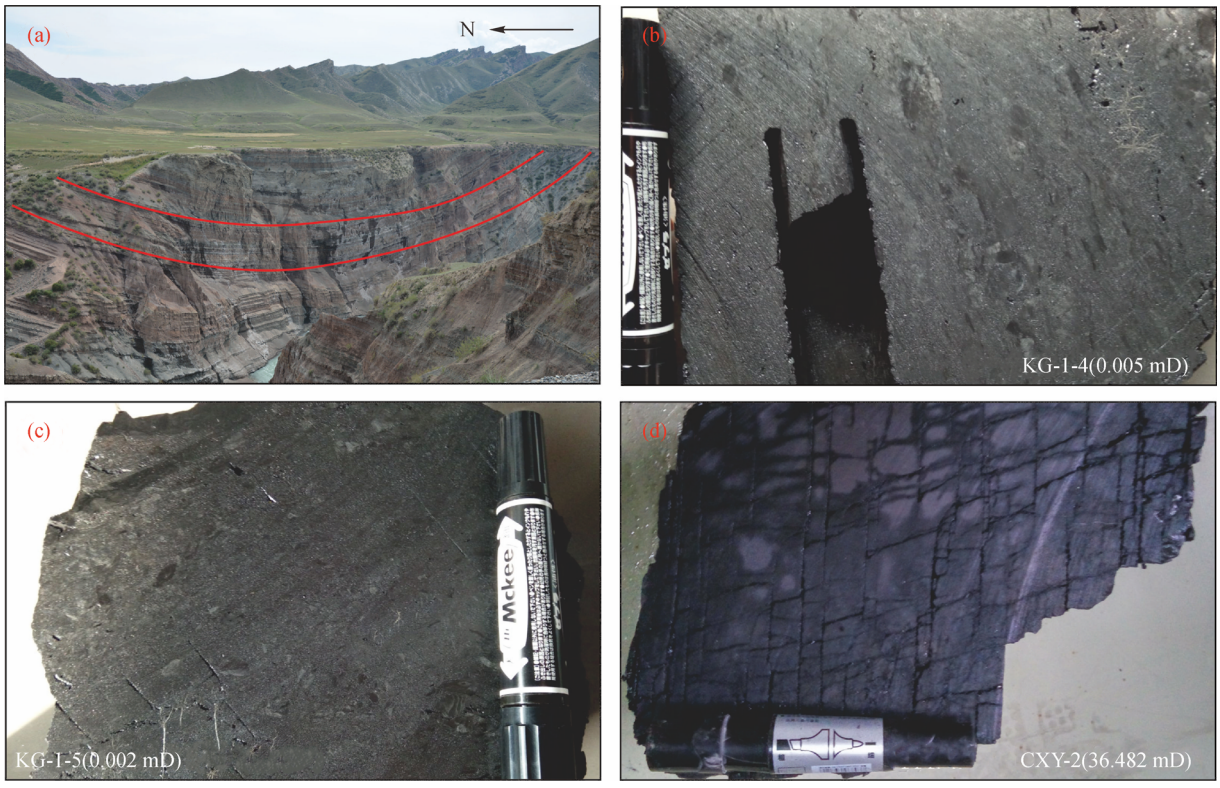

Fig. 6 The synclinal axis of Qingshuihe nearby Hububi River (a) and the characteristics of fracture and permeability of Xishanyao coals in different zones (b), (c), (d).

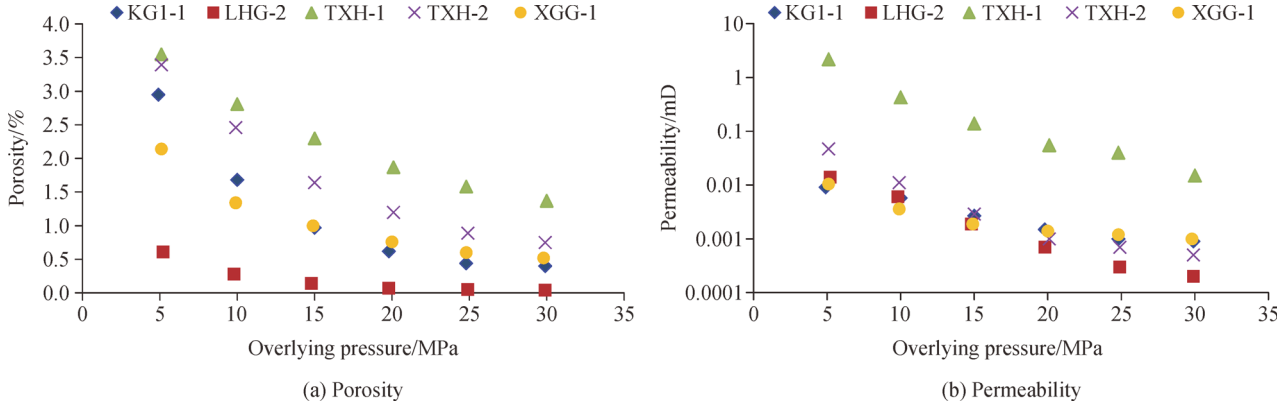

Fig. 7 Relationships between porosity, permeability and overburden pressure of low-rank coals in the middle part of southern Junggar Basin.

4.4 Influence of hydrodynamic condition on gas content

The groundwater flowing in coal-bearing measures has a significant influence on gas content (Wood and Hazra, 2017). In general, the gas content is relatively low in areas with active hydrodynamic conditions. Conversely, the gas content is higher in areas with weak hydrodynamic conditions (Zhang et al., 2015). Based on the results of relevant investigations, the hydrodynamic conditions of groundwater play a direct role in the liquid pressure distribution and fluid migration, which further affects CBM preservation and gas content change by disrupting the balance between adsorption gas, dissolution gas, and free gas (Song et al., 2015; Sun et al., 2019).

4.4.1 Flow pathways of groundwater vs. gas content

The groundwater flow patterns in this study area are

usually expressed as upstream recharge, midstream runoff, and downstream discharge (Fu et al., 2019). The groundwater chemical parameters and hydrodynamic parameters were systematically collated from the geological survey reports covering 25 coal mines in the study area (Table 2). Specifically, the chemical parameters mainly include total dissolved solids (TDS) value along with major ion concentration, while the hydrodynamic parameters include water head height (H), specific yield, and permeability coefficient (K). The H values in the Middle Jurassic Xishanyao coals vertically vary from 712.0 m to 1784.3 m with an average value of 1431.3 m. The TDS value is in the range between 338 mg/L and 30509 mg/L, and the average value is 3436.2 mg/L. In addition, the change interval of the specific yield is between 0.000073 $L \cdot s^{-1} \cdot m^{-1}$ and 2.155 $L \cdot s^{-1} \cdot m^{-1}$ with an average value of 0.255 $L \cdot s^{-1} \cdot m^{-1}$. K spatially ranges from 0.00067 m/day to 1.240 m/day, with an average value of 0.263 m/day (Table 2). The results show that the TDS value increases with decreasing H, and the water type gradually changes from $SO_4 \cdot HCO_3$-Na and $HCO_3 \cdot SO_4$-Na in the western region (Manas-Hutubi) to Cl $\cdot SO_4$-Na and HCO_3°Cl$\cdot SO_4$-Na in the eastern region (Miquan).

Affected by the differences in topography and H, the groundwater migration in the study area is directed from south to north and from west to east, thus forming several water catchment centers with high salinity in the Liuhuanggou and Miquan areas. From south to north and from west to east, the TDS values present an upward trend, which is consistent with the downward trend in H values (Fig. 8). It can be predicted that a groundwater region with a low H value can easily form a stagnant zone with high TDS values. The changes in H values and main ion concentrations, including Cl^-, SO_4^{2-}, and HCO_3^-, show that the direction of groundwater migration is also from west to east. The TDS values in the Manas-Hutubi area are relatively low ranging from 338 mg/L to 3808 mg/L, whereas those in the Liuhuanggou area are usually high in the range between 4464 mg/L and 10292 mg/L. The maximum TDS values are found in the Miquan area ranging from 20024 mg/L to 30509 mg/L (Table 2, Fig. 8). Groundwater activity is the consequence of the combined effects of the east–west and the north–south flows. Therefore, the Urumqi-Miquan in the eastern region is a stagnant zone as well as a CBM enrichment zone, which is associated with the influence of the Urumqi-Miquan strike-slip fault (Fu et al., 2019).

4.4.2 Gas genetic type and stable isotopic values of methane

The CBM desorption gases of three CBM wells from the L-10-1 well in Liuhuanggou, the CS-2 well in Hutubi, and the MM-1 well in Manas are tested to determine the carbon isotope of methane gas. The methane carbon isotopes in the desorption gases in L-10-1 well (coal depth of 461.32–665.82 m), CS-2 well (coal depth of 896.74–1038.14 m), and MM-1 well (coal depth of 1156–1256.5 m) range from –68.23 ‰ to –56.19 ‰, from –55.2 ‰ to –50.7 ‰, and from –47 ‰ to –41.5 ‰, respectively. The relevant results show that as the coal seam depth increases, the methane carbon isotope gradually increases from light to heavy

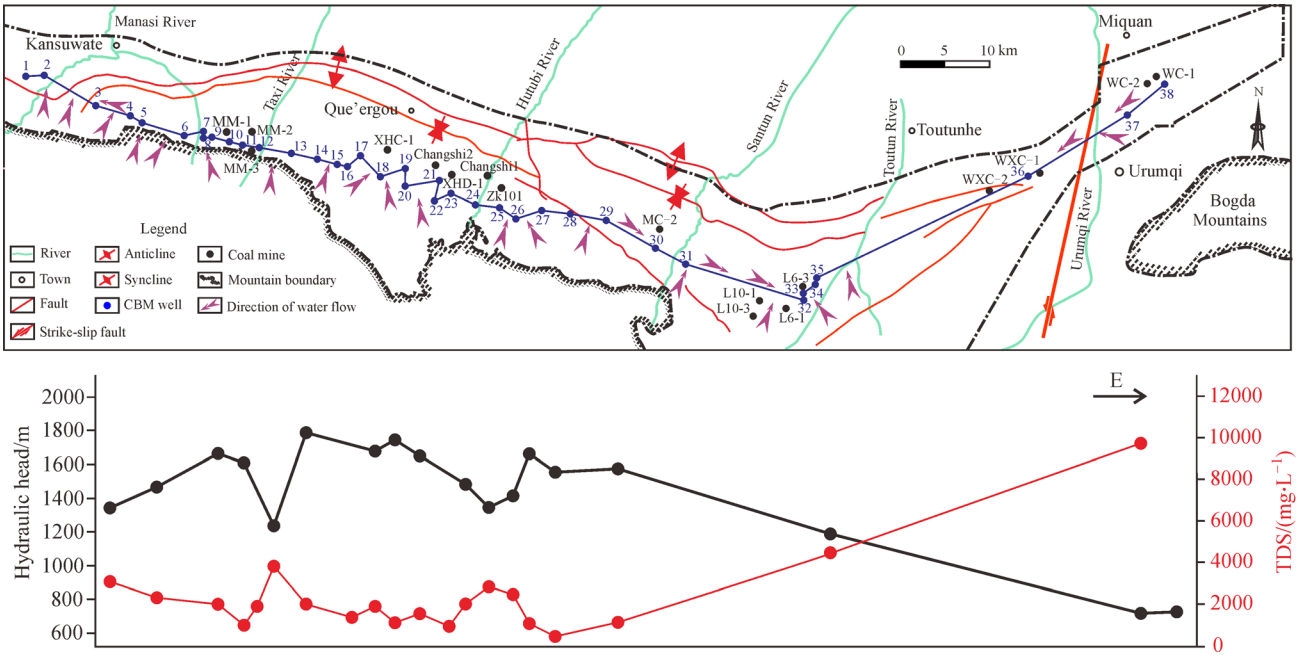

Fig. 8 The total dissolved solids (TDS) values and flow pathways of groundwater in the middle section of the southern Junggar Basin.

Table 2 Hydrogeological parameter statistics for the middle section of the southern Junggar Basin

Number	Coal mine	H/m	Specific yield/ ($L \cdot s^{-1} \cdot m^{-1}$)	K/ ($m \cdot d^{-1}$)	Cl^-/ ($mg \cdot L^{-1}$)	HCO_3^-/ ($mg \cdot L^{-1}$)	SO_4^{2-}/ ($mg \cdot L^{-1}$)	Water type	TDS/ ($mg \cdot L^{-1}$)
3	DBYG	1345.0	0.098	0.130	306.3	1015.7	238.7	$HCO_3 \cdot SO_4$-Na	3075.0
5	XBYG	1457–1463	n	n	304.9	675.8	931.8	$SO_4 \cdot HCO_3 \cdot$Cl-Na	2318.3
8	TW	1660.0	n	n	85.1	604.1	941.4	$SO_4 \cdot HCO_3$-Na·Mg	1975.4
10	DX	1609.0	0.00067–0.008	0.001–0.0436	57.3	647.8	256.2	$HCO_3 \cdot SO_4$-Na	983.9
11	XD	n	0.003	0.002	48.2	469.9	1025.4	$SO_4 \cdot HCO_3$-Na·Ca·Mg	1886.8
12	TXH*	1409–1415	1.240	n	104.0	893.7	306.4	$HCO_3 \cdot SO_4$-Na	3808.0
13	LBW	1784.3	0.051	0.048	118.8	970.2	701.2	$HCO_3 \cdot SO_4$-Na	1995.3
15	XG1	n	n	n	37.2	524.8	3769.3	$SO_4 \cdot HCO_3$-Na·Mg	1354.0
17	XGG	1670.0	n	n	92.2	571.5	896.6	$SO_4 \cdot HCO_3$-Na	1878.2
18	XDG	1745.2	0.206	0.233	59.4	538.1	420.3	$SO_4 \cdot HCO_3$-Na·Mg	1119.2
20	BYS*	1643–1656	0.853	1.318	184.0	646.2	306.4	$HCO_3 \cdot SO_4$-Na	1324–1663
21	FY	n	0.855	1.469	184.0	646.2	306.4	$HCO_3 \cdot SO_4$-Na	n
22	SHG	n	n	n	96.2	813.9	58.4	HCO_3-Na	922.0
23	KG	1482.6	0.234	0.142	335.9	467.6	720.4	$SO_4 \cdot HCO_3 \cdot$Cl-Na	2024.5
24	106T1	1344.1	0.005	0.0	1054.7	260.9	576.4	Cl·SO_4-Na	2819.1
25	106T2	1413.4	0.005	0.003	735.9	171.3	723.0	$SO_4 \cdot Cl^-$Na	2450.3
26	WZG*	1599–1723	n	n	47.0	370.7	461.1	$SO_4 \cdot HCO_3$-Na·Ca·Mg	1010–1100
27	STZXG	1534–1569	n	n	24.8	265.4	216.1	$SO_4 \cdot HCO_3$-Ca·Na	338–558
28	STZDG	n	n	n	17.7	329.5	163.3	$HCO_3 \cdot SO_4$-Na·Ca·Mg	n
29	MDG	1571.1	0.008	0.009	102.8	433.2	403.5	$SO_4 \cdot HCO_3$-Na·Ca	1109.8
35	JY	1184.4	0.004	0.007	n	n	n	Cl·SO_4-Na	4464.0
36	LJM*	n	0.001	0.027	36–430	336–756	769–1896	$SO_4 \cdot HCO_3 \cdot$Cl-Na	n
37	DHG*	712.0	n	n	1666–3414	3001–4144	563–702	$HCO_3 \cdot$Cl·SO_4-Na	7449–11980
38	MQ*	723.0	n	n	9146–14,514	3898–4984	933–1096	Cl·$HCO_3 \cdot SO_4$-Na	20,024–30,509

Notes: n, no data; *, data collected from Fu et al. (2017); H, hydraulic head; K, permeability coefficient; TDS, total dissolved solids; DBYG = Dabaiyanggou; XBYG = Xiaobaiyanggou; TW = Tianwei; DX = Dexiang; XD = Xingda; TXH = Taxihe; LBW = Laobawan; XG1 = Xigou1; XGG = Xiaogangou; XDG = Xiaodonggou; BYS = Baiyangshu; FY = Fengyuan; SHG = Sanhonggou; KG = Kuangou; 106T1 = 106tuan1; 106T2 = 106tuan2; WZG = Weizigou; STZXG = Shitizixigou; STZDG = Shitizidonggou; MDG = Madaogou; JY = Jianyu; LJM = Laojunmiao; DHG = Dahonggou; MQ = Miquan.

(Fig. 9), which suggests that the groundwater system has significant effects on the methane content and geochemical characteristics of methane.

There is a positive linear relationship between the methane carbon isotopes and the buried depths across the study area, indicating that different regions in the study area may belong to the same hydrogeological unit. The value of the methane carbon isotope is an important indicator for determining the origin of CBM, with the methane carbon isotope of the biogenic CBM as lower than –55 ‰ (Li et al., 2014b). Owing to the methane carbon isotope of the mixed genetic gas ranging from –60 ‰ and –55 ‰ (Li and Zhang, 2013; Song, 2015), the burial depths of thermogenic gas and mixed genetic gas in Fig. 9 correspond to deeper than 841.4 m and 841.4–661.6 m, respectively. Considering the high gas content corresponding to burial depths between 600 m and 800 m (Fig. 3), the buried depth interval of the coal seam between 600 m and 850 m is a high gas content area with mixed genetic gas from the Xishanyao Formation. This interval should be the favorable horizon for CBM exploration in the study area.

4.5 CBM enrichment model in the multi-coal seams superimposed region

Based on the structural conditions, hydrogeological conditions, and lithological distribution, previous research has summarized the CBM accumulation models of the Jurassic Badaowan Formation and Xishanyao Formation in the southern Junggar Basin into the following three categories: 1) the monocline accumulation model, 2) the broad and gentle fold accumulation model, and 3) the imbricated thrusting accumulation model (Fu et al., 2017). However, all the CBM enrichment models above are directly related to the fluid pressure in the Middle Jurassic strata. Hence, a monocline structure is adopted as an example to discuss the low rank CBM enrichment model in this multi-coal seams developed area.

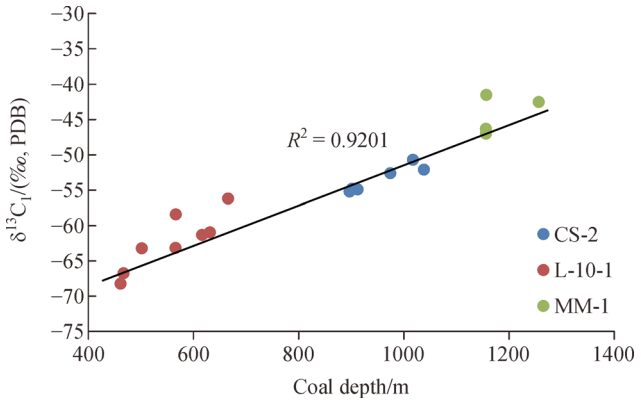

Fig. 9 Relationship between coal depth and $\delta^{13}C_1$ of methane from three CBM wells.

The Xishanyao Formation in the study area is mainly recharged by the Tianshan snow water, surface water, and atmospheric precipitation (Fu et al., 2017, 2019). The groundwater in coal-bearing measures can be vertically divided into three parts: recharge area, runoff area, and stagnant area (Fig. 10). Thus, the CBM enrichment region can also be divided into three stages, namely, the biogenic gas of segment A with a shallow buried depth (< 600 m), the mixed genetic gas of segment B with a medium buried depth (600–850 m), and the thermogenic gas of segment C with a buried depth deeper than 850 m. For segment A, the methane content of the adsorption state is lower, which is attributed to shallower depths and lower reservoir pressures. The dissolved gas strongly increases from the transformation of the part adsorbed methane and free methane due to the low salinity of groundwater and the high methane solubility at this stage, which results in the highest dissolved gas but relatively low gas content. For stage B, with buried depths ranging from 600 m to 850 m, the adsorbed methane content increases significantly with the increase in reservoir pressure. These buried depths are influenced by both secondary biogenic gas migrating from the shallow part and free gas migrated from the deep part, thus resulting in a relatively high gas content (Fig. 10). For segment C with greater buried depths, the absorbed gas content partially decreases because of the higher reservoir temperature, which leads to the transformation of adsorbed methane to free methane. A part of the free gas migrates upward under reservoir pressure to further supply gas

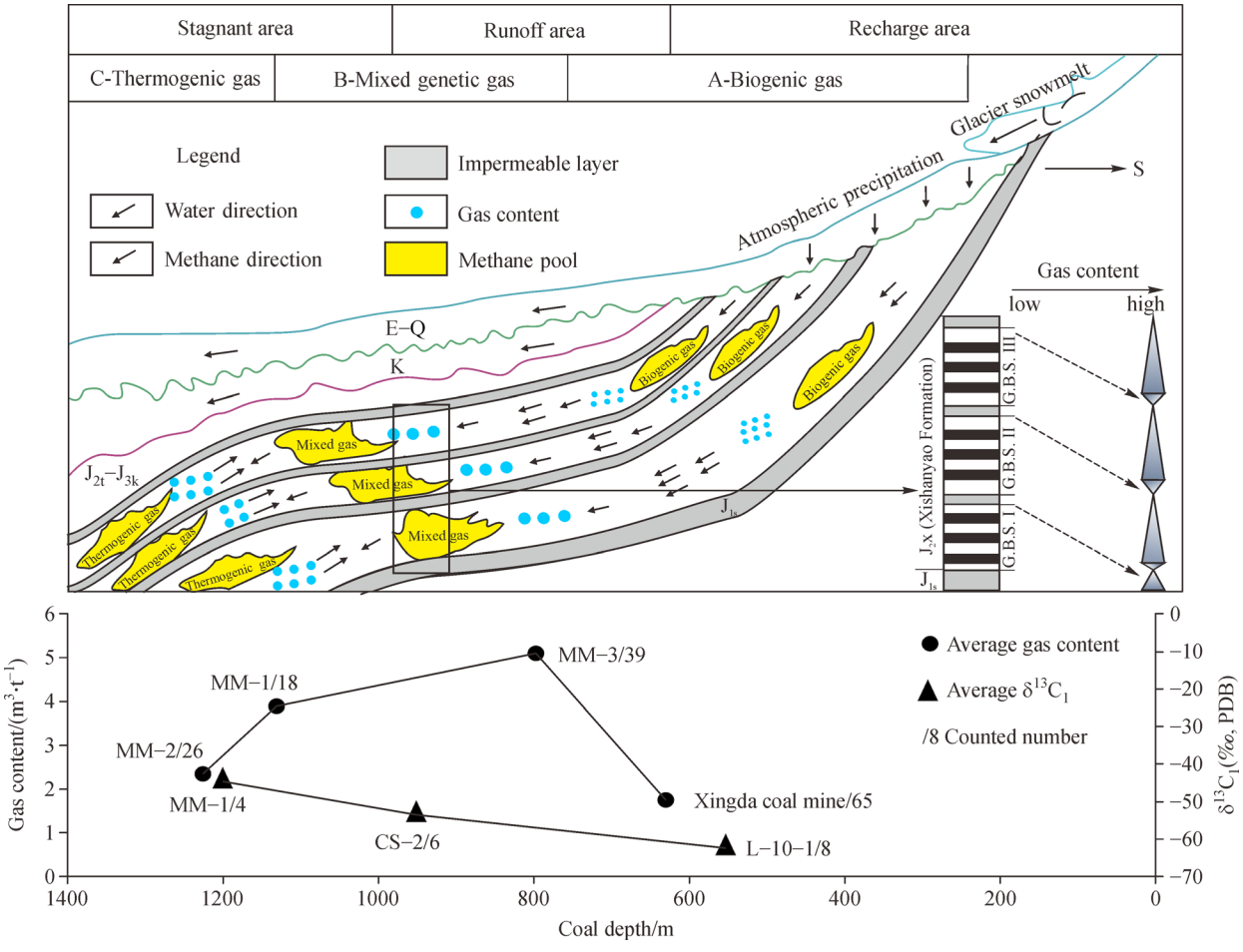

Fig. 10 The CBM enrichment model for a multi-coal seams superimposed region in the middle part of southern Junggar Basin.

content in stage B. Thus, the genesis of CBM in this deep buried depth is dominated by thermogenic gas with a gas content lower than that of segment B (Fig. 10).

Overall, with the increase in the buried depth, the gas content tends to first increase and then decrease. From the perspective of gas content variation, 850 m is the critical burial depth between shallow and deep CBM. The gas contents in the shallow and deep Xishanyao coals are mainly controlled by the reservoir (fluid) pressure and reservoir temperature, respectively. Furthermore, the reservoir pressure is closely linked to the depth of the coal seam and the salinity of the strata water. For a single gas-bearing system at a medium buried depth, the gas content generally increases with increasing strata pressure and burial depth, and the mudstone aquifuge separating each gas-bearing system is usually developed at the end of the highstand system tract. It should be noted that the local variation of gas content in each gas-bearing system is also weakly affected by the lithology of the surrounding rocks.

This CBM accumulation model of multi-coals mixed genetic gas can also be extended to other coal-bearing regions with similar geological conditions. Furthermore, the two conditions should be considered first including medium-low rank coals and multi-coals developments. Biogenic gas is mainly found in medium-low rank coals (Pashin et al., 2014; Fu et al., 2019), and at least six coal seams and two coal-bearing gas systems are necessary in multi-coal superimposed regions. In addition, the favorable exploration depths should be specifically discussed in other regions owing to different geological conditions.

5 Conclusions

1) The gas content of the Xishanyao coals first increases and then decreases with increasing buried depth, and the maximum gas content appears at the depth of 600–850 m. The gas contents with shallower depths are controlled by strata pressure whereas those with deeper depths are dominated by the negative effect of reservoir temperature.

2) The Middle and Lower Xishanyao Formation can be vertically divided into three independent gas-bearing systems. Thick mudstone aquifuges separating different gas-bearing systems are usually developed at the end of the highstand system tracts. For each gas-bearing system, the gas content increases with the increase in reservoir pressure. In addition, the gas content is also partially affected by the lithology of the surrounding rocks.

3) Affected by both the topography and the water head height, the migration directions of groundwater in the study area are generally from south to north and from west to east, finally forming high-salinity water catchment centers in the Liuhuanggou and Miquan areas. Furthermore, the TDS values in the groundwater show an upward trend from south to north and from west to east, which is attributed to the various H values and the Urumqi-Miquan strike-slip fault.

4) A CBM accumulation model of the multi-coal mixed genetic gas is established considering a monoclinal structure combined with depositional environments, geological tectonics, and hydrogeological conditions. The change of gas content in the shallow and deep Xishanyao coals is mainly controlled by the reservoir (fluid) pressure and reservoir temperature, respectively. The burial depth interval between 600 m and 850 m presents the highest gas content owing to the joint influence of thermogenic gas and biogenic gas, which would be a favorable CBM exploration horizon in the southern Junggar Basin.

Acknowledgements This research paper was supported by the China Geological Survey Project (DD20160204-3), the Discipline Innovation Team of Liaoning Technical University (LNTU20TD-05; LNTU20TD-14; LNTU20TD-30), the Guiding Program of Liaoning Natural Science Founds (2019-ZD-0046), and the Scientific Research Funding Project of Liaoning Education Department (LJ2019JL004).

References

Ayers W B J (2002). Coalbed gas systems, resources, and production and a review of contrasting cases from the San Juan and Powder River basins. AAPG Bull, 86(11): 1853–1890

Chen B T, Yu X H, Wang T Q, Pan S X, Yang L S, Tan C P, Li S L (2014). Characteristics of sequence stratigraphy and coal enrichment controlling factors of lower-middle Jurassic coal-bearing series, south margin of Junggar Basin, NW China. Acta Sedimentol Sin, 32(1): 61–67 (in Chinese)

Chen Y, Ma D M, Fang S Y, Guo C, Yang F, Hou D Z (2019). Enrichment and high-yield models of coalbed methane influenced by geologic structures and hydrologic conditions. J Xi'an Univ Sci Tech, 39(4): 644–655 (in Chinese)

Chen Y, Tang D Z, Xu H, Li Y, Meng Y J (2015). Structural controls on coalbed methane accumulation and high production models in the eastern margin of Ordos Basin, China. J Nat Gas Sci Eng, 23: 524–537

Cienfuegos P, Loredo J (2010). Coalbed methane resources assessment in Asturias (Spain). Int J Coal Geol, 83(4): 366–376

Fu H J, Tang D Z, Pan Z J, Yan D T, Yang S G, Zhuang X G, Li G Q, Chen X, Wang G (2019). A study of hydrogeology and its effect on coalbed methane enrichment in the southern Junggar Basin, China. AAPG Bull, 103(1): 189–213

Fu H J, Tang D Z, Xu H, Xu T, Chen B L, Hu P, Yin Z Y, Wu P, He G J (2016). Geological characteristics and CBM exploration potential evaluation: a case study in the middle of the southern Junggar Basin, NW China. J Nat Gas Sci Eng, 30: 557–570

Fu H J, Tang D Z, Xu T, Xu H, Tao S, Zhao J L, Chen B L, Yin Z Y (2017). Preliminary research on CBM enrichment models of low-rank coal and its geological controls: a case study in the middle of the southern Junggar Basin, NW China. Mar Pet Geol, 83: 97–110

Fu H J, Yan D T, Yang S G, Wang X M, Zhuang Z, Sun M D (2020). Characteristics of *in situ* stress and its influence on coalbed methane

development: a case study in the eastern part of the southern Junggar Basin, NW China. Energy Sci Eng, 8(2): 515–529

Hamilton S K, Esterle J S, Golding S D (2012). Geological interpretation of gas content trends, Walloon Subgroup, eastern Surat Basin, Queensland, Australia. Int J Coal Geol, 101: 21–35

Hou H H, Shao L Y, Guo S Q, Li Z, Zhang Z J, Yao M L, Zhao S, Yan C Z (2017). Evaluation and genetic analysis of coal structures in deep Jiaozuo Coalfield, northern China: investigation by geophysical logging data. Fuel, 209: 552–566

Hou H H, Shao L Y, Tang Y, Li Y N, Liang G D, Xin Y L, Zhang J Q (2021). Coal seam correlation in terrestrial basins by sequence stratigraphy and its implications for palaeoclimate and palaeoenvironment evolution. J Earth Sci

Hou H H, Shao L Y, Tang Y, Zhao S, Yuan Y, Li Y N, Mu G Y, Zhou Y, Liang G D, Zhang J Q (2020). Quantitative characterization of low-rank coal reservoirs in the southern Junggar Basin, NW China: Implications for pore structure evolution around the first coalification jump. Mar Pet Geol, 113: 104165

Hou H H, Shao L Y, Wang S, Xiao Z H, Wang X T, Li Z, Mu G Y (2019). Influence of depositional environment on coalbed methane accumulation in the Carboniferous-Permian coal of the Qinshui Basin, northern China. Front Earth Sci, 13(3): 535–550

Li G H (2016). Coal reservoir characteristics and their controlling factors in the eastern Ordos Basin in China. Int J Min Sci Technol, 26(6): 1051–1058

Li G H, Zhang H (2013). The origin mechanism of coalbed methane in the eastern edge of Ordos Basin. Sci China Earth Sci, 56(10): 1701–1706

Li M H, Li Z D, Liao J D (2005). Analysis of ground stress in the southern part of the Junggar Basin and discussion of the related issues. Xinjiang Geol, 23(4): 343–346 (in Chinese)

Li M, Jiang B, Lin S F, Lan F J, Wang J L (2013). Structural controls on coalbed methane reservoirs in Faer coal mine, southwest China. J Earth Sci, 24(3): 437–448

Li W, Wang X K, Zhang B J, Chen Z X, Pei S Q, Yu Z C (2020). Large-scale gas accumulation mechanisms and reservoir-forming geological effects in sandstones of central and western China. Pet Explor Dev, 47(4): 714–725

Li X, Fu X H, Yang X S, Ge Y Y, Quan F K (2018a). Coalbed methane accumulation and dissipation patterns: a case study of the Junggar Basin, NW China. J Asian Earth Sci, 160: 13–26

Li Y J, Shao L Y, Eriksson K A, Tong X, Gao C X, Chen Z S (2014a). Linked sequence stratigraphy and tectonics in the Sichuan continental foreland basin, Upper Triassic Xujiahe Formation, southwest China. J Asian Earth Sci, 88: 116–136

Li Y N, Shao L Y, Hou H H, Tang Y, Yuan Y, Zhang J Q, Shang X X, Lu J (2018b). Sequence stratigraphy, palaeogeography, and coal accumulation of the fluvio-lacustrine Middle Jurassic Xishanyao Formation in central segment of southern Junggar Basin, NW China. Int J Coal Geol, 192: 14–38

Li Y, Tang D Z, Fang Y, Xu H, Meng Y J (2014b). Distribution of stable carbon isotope in coalbed methane from the east margin of Ordos Basin. Sci China Earth Sci, 57(8): 1741–1748

Li Y, Yang J H, Pan Z J, Meng S Z, Wang K, Niu X L (2019). Unconventional natural gas accumulations in stacked deposits: a discussion of Upper Paleozoic coal-bearing strata in the east margin of the Ordos Basin, China. Acta Geolo Sin-Engl, 93(1): 111–129

Liu D M, Wang Y J, Cai Y D (2018). Main controlling geological factors and accumulation model analysis of low-rank CBM enrichment. Coal Sci Tech, 46(6): 1–8 (in Chinese)

Lv Y M, Tang D Z, Xu H, Luo H H (2012). Production characteristics and the key factors in high-rank coalbed methane fields: a case study on the Fanzhuang Block, Southern Qinshui Basin, China. Int J Coal Geol, 96–97: 93–108

Moore T A (2012). Coalbed methane: a review. Int J Coal Geol, 101: 36–81

Ouyang Y L, Sun B, Wang B, Tian W G, Zhao Y, Cao H X (2017). CBM sealing system and its relationship with CBM enrichment. Nat Gas Ind B, 4(1): 39–47

Pan J N, Zhao Y Q, Hou Q L, Jin Y (2015). Nanoscale pores in coal related to coal rank and deformation structures. Transp Porous Media, 107(2): 543–554

Pashin J C, Groshong R H Jr (1998). Structural control of coalbed methane production in Alabama. Int J Coal Geol, 38(1–2): 89–113

Pashin J C, Mcintyre-Redden M R, Mann S D, Kopaska-Merkel D C, Varonka M, Orem W (2014). Relationships between water and gas chemistry in mature coalbed methane reservoirs of the Black Warrior Basin. Int J Coal Geol, 126(2): 92–105

Qin Y, Moore T A, Shen J, Yang Z B, Shen Y L, Wang G (2018). Resources and geology of coalbed methane in China: a review. Int Geol Rev, 60(5–6): 777–812

Scheltens M, Zhang L F, Xiao W J, Zhang J J (2015). Northward subduction-related orogenesis of the southern Altaids: constraints from structural and metamorphic analysis of the HP/UHP accretionary complex in Chinese southwestern Tianshan, NW China. Geoscience Frontiers, 6(2): 191–209

Shao L Y, Hou H H, Tang Y, Lu J, Qiu H J, Wang X T, Zhang J Q (2015). Selection of strategic replacement areas for CBM exploration and development in China. Nat Gas Ind B, 2(2–3): 211–221

Shen Y L, Qin Y, Wang G G X, Guo Y H, Shen J, Gu J Y, Xiao Q, Zhang T, Zhang C L, Tong G C (2017). Sedimentary control on the formation of a multi-superimposed gas system in the development of key layers in the sequence framework. Mar Pet Geol, 88: 268–281

Song G (2015). Simulation research on biogenic and thermogenic gas from brown coal in Dananhu depression of Tuha Basin. Dissertation for Master's Degree. Xuzhou: China University of Mining and Technology (in Chinese)

Song Y, Li Z, Jiang L, Hong F (2015). The concept and the accumulation characteristics of unconventional hydrocarbon resources. Petrol Sci, 12(4): 563–572

Song Y, Liu H L, Hong F, Qin S F, Liu S B, Li G Z, Zhao M J (2012). Syncline reservoir pooling as a general model for coalbed methane (CBM) accumulations: mechanisms and case studies. J Petrol Sci Eng, 88–89: 5–12

Song Y, Liu S B, Ma B Z, Li J W, Ju Y W, Li G Z, Yang Z Y (2016). Research on formation model and geological evaluation method of the middle to high rank coalbed methane enrichment and high production area. Earth Sci Front, 23(3): 1–9 (in Chinese)

Sun D, Liu X Z, Yang H J, Cao N, Zhang Z P, Chen Y S, Li D M (2019). Analysis of hydrogeological characteristics and water environmental impact pathway of typical shale gas exploration and development

zones in Sichuan Basin, China. J Groundw Sci Eng, 7(3): 195–213

Sun Z M, Shen J (2014). Bogda nappe structure and its relations to hydrocarbon in Xinjiang. Petrol Geol & Exp, 36(4): 429–434 (in Chinese)

Tang Y (2020). Research on layer selection method for fracturing of multi-layer superimposed CBM system in the southern Junggar Basin. Dissertation for Doctor's Degree. Beijing: China University of Geosciences (Beijing) (in Chinese)

Wang K X (2019). Research on main geological controls and enrichment model of coalbed methane distribution in China. Earth Env Sci, 300: 022071

Wood D A, Hazra B (2017). Characterization of organic-rich shales for petroleum exploration & exploitation: a review. Part 3: applied geomechanics, petrophysics and reservoir modeling. J Earth Sci, 28 (5): 779–803

Xiao X M, Wei Q, Gai H F, Li T F, Wang M L, Pan L, Chen J, Tian H (2015). Main controlling factors and enrichment area evaluation of shale gas of the Lower Paleozoic marine strata in south China. Petrol Sci, 12(4): 573–586

Yang Z B, Qin Y, Wang G X, An H (2015). Investigation on coal seam gas formation of multi-coalbed reservoir in Bide-Santang Basin, Southwest China. Arab J Geosci, 8(8): 5439–5448

Yao Y B, Liu D M, Yan T (2014). Geological and hydrogeological controls on the accumulation of coalbed methane in the Weibei field, southeastern Ordos Basin. Int J Coal Geol, 121: 148–159

Yuan Y, Shan Y S, Tang Y, Cao D Y (2020). Coalbed methane enrichment regularity and major control factors in the Xishanyao Formation in the western part of the southern Junggar Basin. Acta Geolo Sin-Engl, 94(2): 485–500

Yuan Y, Tang Y, Shan Y S, Zhang J Q, Cao D Y, Wang A M (2018). Coalbed methane reservoir evaluation in the Manas Mining area, Southern Junggar Basin. Energ Explor Exploit, 36(1): 114–131

Zhang Z, Qin Y, Fu X H, Yang Z B, Guo C (2015). Multi-layer superposed coalbed methane system in southern Qinshui Basin, Shanxi Province, China. J Earth Sci, 26(3): 391–398

Zou C N, Yang Z, Zhu R K, Zhang G S, Hou L H, Wu S T, Tao S Z, Yuan X J, Dong D Z, Wang Y M, Wang L, Huang J L, Wang S F (2015). Progress in China's unconventional oil & gas exploration and development and theoretical technologies. Acta Geolo Sin-Engl, 89 (3): 938–971